

RSC Advances



This is an *Accepted Manuscript*, which has been through the Royal Society of Chemistry peer review process and has been accepted for publication.

Accepted Manuscripts are published online shortly after acceptance, before technical editing, formatting and proof reading. Using this free service, authors can make their results available to the community, in citable form, before we publish the edited article. This *Accepted Manuscript* will be replaced by the edited, formatted and paginated article as soon as this is available.

You can find more information about *Accepted Manuscripts* in the [Information for Authors](#).

Please note that technical editing may introduce minor changes to the text and/or graphics, which may alter content. The journal's standard [Terms & Conditions](#) and the [Ethical guidelines](#) still apply. In no event shall the Royal Society of Chemistry be held responsible for any errors or omissions in this *Accepted Manuscript* or any consequences arising from the use of any information it contains.

Cite this: DOI: 10.1039/c0xx00000x

www.rsc.org/xxxxxx

ARTICLE TYPE

Post-isomorphic substitution of trivalent metal cations for Ca²⁺ in portlandite crystals

Man Park,^{*a} Jun Hyung Kim,^a Ahmad Imran,^a Min-Cheol Choi,^a Kwang Seop Kim^a and Sridhar Komarneni^b

Received (in XXX, XXX) Xth XXXXXXXXX 20XX, Accepted Xth XXXXXXXXX 20XX
DOI: 10.1039/b000000x

Isomorphic substitution, position replacement of one cation by another of similar size, leads to incorporation of a variety of cations into solid crystals without any significant changes to the primary crystal structures. To date, isomorphic substitution has been known to take place almost exclusively via co-crystallization of the cations during formation of the crystals. We report here the discovery of isomorphic substitution of trivalent metal cations for Ca²⁺ ions in portlandite crystals at room temperature as evidenced by the transient appearance of metastable phase, the formation of Ca-based layered double hydroxides at high pH, the distinct shift of suspension pH after phase transition, and the in situ topochemical reaction. This post-crystallization isomorphic substitution provides an innovative pathway for the synthesis of materials through chemical manipulation of crystals as well as a new insight into interpretation on their weathering and transformation processes.

Introduction

Isomorphic substitution leads to incorporation of a variety of cations into solid crystals without any significant changes to the primary crystal structures, developing diverse chemical functions such as ion exchange, catalysis, electrochemical potential, photosensitivity etc.¹⁻⁴ To date, isomorphic substitution has been known to take place almost exclusively via co-crystallization of the cations during formation of the crystalline structures.⁴⁻⁸ Once crystallized, structural cations are believed to be very difficult to replace mainly due to strong electrostatic repulsion and high lattice energy as long as the primary structures remain intact. Nevertheless, there have been incessant attempts to elucidate the possibility of post-crystallization isomorphic substitution (hereinafter referred to as 'post-isomorphic substitution')^{8,9,10} because it can open a new pathway for materials synthesis as well as for understanding the intriguing chemical processes involved in the formation and transformation of inorganic minerals.

Substantial degree of isomorphic substitution is observed especially in porous minerals such as zeolites,^{4,9} swelling phyllosilicates,^{1,9} layered double hydroxides (LDHs)^{4,6,7} etc. In general, both layered and network structures of silicates are mainly co-crystallized with tetrahedra of various cations through isomorphic substitution. Similarly, octahedral sheets of phyllosilicates are composed exclusively of octahedra of diverse cations. On the other hand, octahedral sheets of LDHs exhibit much more variations in isomorphic substitution of cations than those of phyllosilicates. Heterogeneous polyhedra like tetrahedron¹¹ and decahedron¹² are often co-crystallized in octahedral sheets of LDHs. Consequently, more flexible post-synthesis routes to the incorporation of heterogeneous cations

could be applied to LDHs than zeolites and phyllosilicates, including the chemical transformation processes like reconstruction of oxides into the corresponding LDHs^{13,14} and selective reoxidation of specific framework cations⁷ as well as the recrystallization processes like localized dissolution-recrystallization and curing of structural defects.^{5,9,10}

Our special attention has been given to phase transition of portlandite, calcium hydroxide, not only because coordination number of Ca²⁺ increases from six in portlandite to seven in Ca-based LDHs but also because they occur during hydration of calcium aluminate cement, one of the poorly understood chemical processes.^{12,15,16} Furthermore, Ca-based LDHs are distinguished from other LDHs by unique combination of a capped trigonal antiprismatic decahedral Ca²⁺ with octahedral trivalent cation (M³⁺) at a fixed molar ratio of 2Ca²⁺/M³⁺.^{12,17,18} Typically, a water molecule can occupy the seventh apex of the Ca²⁺-polyhedron to project into interlayer space. Therefore, it can be thermodynamically favorable in portlandite that octahedral M³⁺ ions substitute for one third of octahedral Ca²⁺ ions while adding a water molecule to each of the rest, although the formation mechanism of LDHs had been interpreted solely by co-precipitation.^{4,6} In this study, we demonstrate the post-isomorphic substitution of trivalent metal cations for Ca²⁺ ions in portlandite crystals at room temperature as evidenced by the transient appearance of metastable phase, the formation of Ca-based layered double hydroxides at high pH, the distinct shift of suspension pH after phase transition, and the in situ topochemical reaction.

Experimental

All the chemicals had a high purity of more than analytical grade.

Deionized water was decarbonated by boiling before use. Two different morphologies of portlandite crystals were used in this study; the polyhedral hexagonal tablet crystals were synthesized by hydrothermally treating a mixture of equi-volumes of 1.0 M CaCl_2 and 2.0 M NaOH solutions at 353 K for 2 h whereas the hexagonal platelet ones by mixing equi-volumes of 0.2 M CaCl_2 with 0.4 M NaOH in the presence of 0.1 M of Na_2SO_4 followed by 1 hr stirring.¹⁹ The crystals were separated by filtration, washed with deionized water twice, and dried at 333 K.

Plausibility for phase transition of portlandite into Ca-LDHs via the post-isomorphic substitution was evaluated here by simply reacting portlandite with trivalent cations in aqueous solution at room temperature. An aqueous solution of 0.1 M MCl_3 or $\text{M}(\text{NO}_3)_3$ (M = trivalent metal cation), typically FeCl_3 , was titrated to an aqueous suspension of portlandite (1.48 g/100 mL; equal to 0.2 mole/L) at a flow rate of 0.8 ~ 2.0 mL/min over stirring. The solid phases reacted at various molar ratios of $\text{Ca}^{2+}/\text{M}^{3+}$ were quickly separated by centrifugation for 3 min at 3000 rpm, smeared over slide glass or wide dish, rapidly dried by blowing air, and kept in a tightly capped vessel.

Water solubility of CaFe-LDH was evaluated by measuring the weight of the water-washed CaFe-LDH after equilibrating its suspension (0.2 g/100mL) for 4 h. Powder XRD patterns were recorded at a scanning speed of 3°/min by Ni-filtered Cu K α radiation at 40 kV and 40 mA (Rigaku JP/D/MAX-2200H). Morphology changes were examined with a scanning electron microscope (Hitachi S-570 equipped with EDS) after Pt-coating.

Results and discussion

Reaction with Fe^{3+}

Portlandite was reacted with Fe^{3+} by the addition of 0.1 M FeCl_3 solution at a flow rate of 0.8 mL/min while stirring. On addition of Fe^{3+} , the color of the suspension turned brown to indicate the presence of ferric hydroxide species. Changes in the XRD patterns of the solid phases (Fig. 1) and the suspension pH (Fig. 2) were monitored immediately after the addition of Fe^{3+} .

The XRD patterns (Fig. 1) clearly indicated in-situ phase transition of portlandite to CaFe-LDH. All the XRD patterns did not show any peak broadening and base-line drifting which were typically found in reconstruction and recrystallization processes.^{13,14} Relative overall intensity of the peaks assigned to CaFe-LDH increased with the addition of Fe^{3+} while that of those to portlandite decreased correspondingly. It was remarkable that the phase transition occurred immediately and almost stoichiometrically on adding Fe^{3+} regardless of the molar ratio of $\text{Ca}^{2+}/\text{Fe}^{3+}$. As soon as portlandite reacted with Fe^{3+} , a proportion of portlandite corresponding to a ratio of $\text{Ca}^{2+}/\text{Fe}^{3+}$ was almost promptly converted into CaFe-LDH. When Fe^{3+} solution was rapidly added into the portlandite suspension (above a flow rate of ca. 2 mL/min), a highly metastable CaFe-LDH phase appeared transiently with a basal spacing of 1.028 nm (Fig. S1). This phase was quickly converted into the typical CaFe-LDH phase (chloride form with a basal peak at 0.78 nm or nitrate form at 0.86 nm) even in air-dried state. This phase seemed to be highly hydrated¹⁸ or intercalated with $[\text{Fe}(\text{OH})_4]^-$ like the $[\text{Al}(\text{OH})_4]^-$ -intercalated AFm phases.¹⁵ These results strongly suggested in-situ transformation of portlandite into CaFe-LDHs via the post-

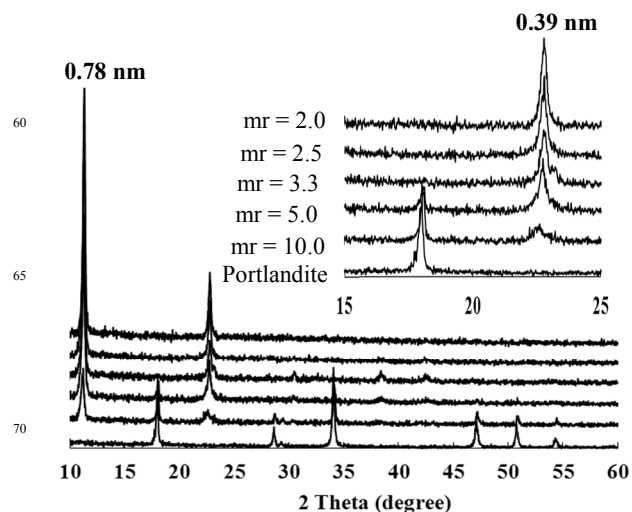


Figure 1. XRD patterns of the solid phases monitored immediately after the addition of Fe^{3+} at a flow rate of 0.8 mL/min (mr = molar ratio of $\text{Ca}^{2+}/\text{Fe}^{3+}$).

isomorphic substitution of Fe^{3+} for Ca^{2+} rather than localized dissolution-recrystallization route.

A supporting evidence for the post-isomorphic substitution was further provided by the change of the suspension pH during and after the titration of Fe^{3+} (Fig. 2). The pH curve during the titration revealed two distinct regions, an initial slow decrease followed by a steep drop, which were then followed by a plateau region after the end of titration. The first slow decrease region could be explained by the reactions (I) and (I'), formation of metal hydroxide species,^{6,20} and the reactions (II) and (II'), incorporation of $[\text{M}(\text{OH})_4]^-$ into portlandite via the post-isomorphic substitution for Ca^{2+} .

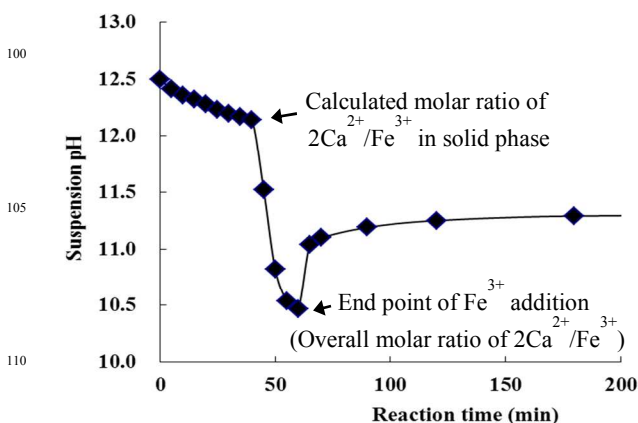
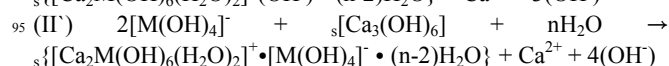
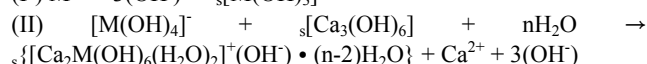
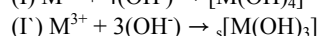
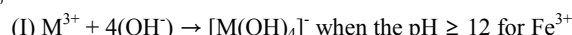


Figure 2. Change in the suspension pH monitored immediately after the addition of Fe^{3+} at a flow rate of 0.8 mL/min.

(III) $s\{[\text{Ca}_2\text{M}(\text{OH})_6(\text{H}_2\text{O})_2]^+(\text{OH})^- \cdot (n)\text{H}_2\text{O}\} + x\text{A}^- \rightarrow s\{[\text{Ca}_2\text{M}(\text{OH})_6(\text{H}_2\text{O})_2]^+(\text{OH})_{1-x}(\text{A}^-)_x \cdot (n\text{H}_2\text{O})\} + x(\text{OH})^-$, where subscript 's' means 'solid'.

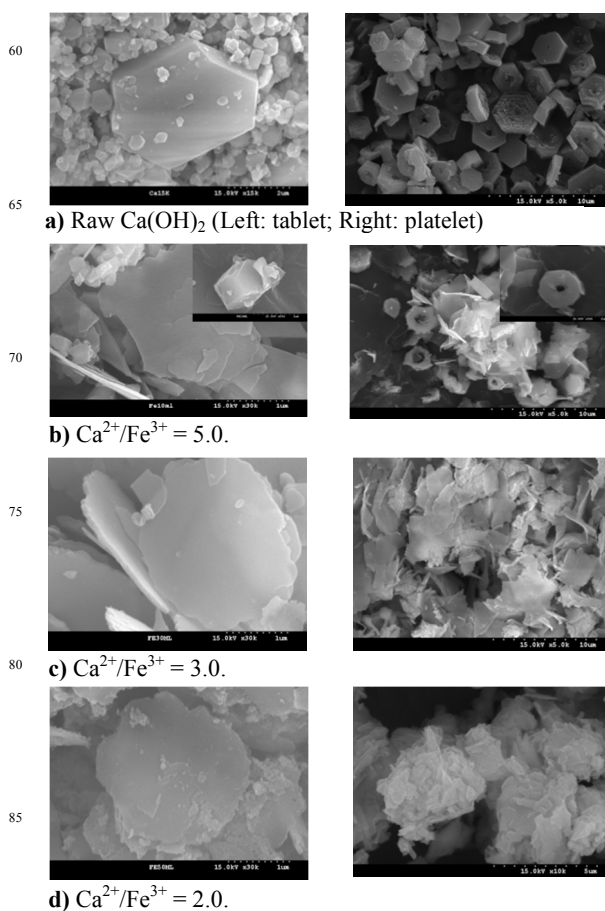
5 Decrease in pH by the reactions (I) and possibly (I') could be buffered by the corresponding release of OH⁻ by the reactions (II) and (II') and eventually the reaction (III), hydroxide exchange by counter anion. The reaction (II') was suggested from the transient appearance of the metastable phase. Interestingly, both the in-situ
 10 phase transition and the transient appearance could be reasonably explained by rapid intercalation of [Fe(OH)₄]⁻ and its prolific substitution for crystallized Ca(OH)₂ moiety of adjacent portlandite layers. As the phase transition progresses, the first slow pH decrease region could be expected from delayed
 15 equilibrium of the reaction (III) and from lower water solubility of CaFe-LDH than that of portlandite.^[16] Here, it was worthy to note that CaFe-LDH was formed at the pH of aqueous Ca(OH)₂-saturated solution, much higher than that of CaFe-LDH suspension (Fig. S2). This higher formation pH is a clear
 20 indication of the post-isomorphic substitution because crystallization of M²⁺M³⁺-LDH frameworks via coprecipitation route takes place below the pH at which a M²⁺ hydroxide precipitates alone.^{6,21} The second steep pH drop region could result mainly from the over-stoichiometric addition of Fe³⁺ that
 25 induces most likely the reaction (I') consuming free OH⁻. As the pH decreases below the point of equilibrium water solubility of CaFe-LDH, its dissolution takes place leading to an increase in pH. Even though there is no excess addition of Fe³⁺, a pH shift would result from the difference in water solubility between
 30 portlandite and CaFe-LDH as soon as portlandite disappears. In addition, over-stoichiometric addition of M³⁺ leads to crystallization of oversaturated Ca²⁺ into CaFe-LDH via the reaction (IV), typical coprecipitation route.

35 (IV) $[\text{M}(\text{OH})_3] + 2\text{Ca}^{2+} + (3-x)(\text{OH})^- + x\text{A}^- + n\text{H}_2\text{O} \rightarrow s\{[\text{Ca}_2\text{M}(\text{OH})_6(\text{A}^-)_x(\text{H}_2\text{O})_2]^+(\text{OH})_{1-x} \cdot (m\text{H}_2\text{O})\}$, where $m = n - (2 - x)$.

Eventually, reactions such as dissolution, coprecipitation and ion
 40 exchange reach an equilibrium leading to a pH plateau, the third region. The sharp pH shift between the regions one and three is also indicative of the post-isomorphic substitution because typical coprecipitation route, the reaction (IV), could not induce any pH shift after the formation of LDHs.^{6,21}

45 The in-situ M³⁺-dependent phase transition excludes both nucleation and crystal growth stages, resulting in the coexistence of portlandite and CaFe-LDH even within one crystal. The substitution of [Fe(OH)₄]⁻ for crystallized Ca(OH)₂ moiety leads to development of positive layer charge that is compensated by
 50 either (OH)⁻ or [Fe(OH)₄]⁻ intercalated through simultaneous expansion of interlayer space. Consequently, the phase transition would take place without any significant changes in crystal morphology during the titration. Fig. 3 shows the changes of crystal morphology during the addition of Fe³⁺.

55 Two distinct shapes of portlandite crystals, one as polyhedral hexagonal tablet and the other as hexagonal platelet¹⁹ were used in this experiment. The pristine tablets were 1~5 μm in diameter and 0.5~1 μm in thickness while the pristine platelets 2~5 μm in



90 **Figure 3.** Scanning electron micrographs of the solid phases reacted with Fe³⁺ at various molar ratios of Ca²⁺/Fe³⁺.

diameter and about 1 μm in thickness. After reaction with Fe³⁺, the tablet crystals were only sliced into thin flakes without any significant changes in diameter. Similarly, the platelet crystals
 95 indicated detachment of thickness-sized strips from the rim surface, and steadily decreased in diameter. A proportion of flakes or strips increased with the molar ratio of Fe³⁺. At higher molar ratio of Ca²⁺/Fe³⁺, it was frequently observed that the flakes or the strips were peeling from the surfaces of the crystals
 100 (the inserted images of in Fig. 3 b). Addition of over-stoichiometric Fe³⁺ resulted in blunting of the crystal outlines surely due to dissolution of CaFe-LDH. At the molar ratio of 2.0 where over-stoichiometric Fe³⁺ was added due to water solubility of portlandite, tiny particulates were frequently observed to
 105 indicate coprecipitation (Fig. 3 d). These results confirm that the phase transition of portlandite into CaFe-LDHs undergoes topochemically as well as stoichiometrically via post-isomorphic substitution.

110 Reactions with other M³⁺ ions.

The reactions with other trivalent cations such as Al³⁺, Ga³⁺, Cr³⁺ and In³⁺ also successfully led to the in-situ topochemical phase transition of portlandite to CaM-LDHs, as shown in Figures 4 and 5. Al³⁺ and Ga³⁺ exhibited the reaction behaviors very similar to
 115 that of Fe³⁺ although each region in their pH curves exhibited the differences in the molar Ca²⁺/M³⁺ ratio and the pH value (Fig. S3).

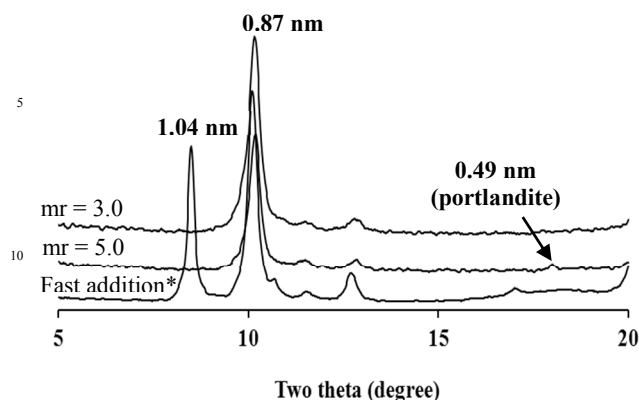


Figure 4. XRD patterns of portlandite reacted with Al^{3+} ($\text{mr} =$ molar ratio of $\text{Ca}^{2+}/\text{Al}^{3+}$). *At an addition rate of 2.0 ml/min at $\text{mr} = 5.0$.

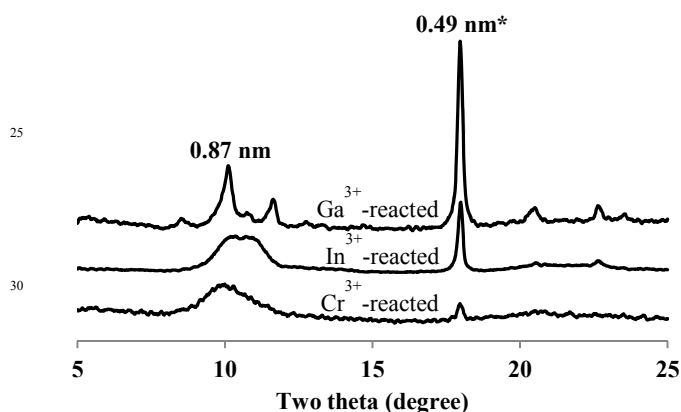


Figure 5. XRD patterns of portlandite reacted with M^{3+} at a molar ratio of $\text{Ca}^{2+}/\text{M}^{3+} = 5.0$.



Figure 6. XRD patterns (a) and scanning electron micrographs (b) of portlandites reacted with Ga^{3+} (i) and with In^{3+} (ii).

These differences mainly resulted from aqueous acidity of each cation. The highly metastable phase was also observed in the XRD patterns of the reaction products obtained by the fast addition of Al^{3+} and Ga^{3+} at the molar $\text{Ca}^{2+}/\text{M}^{3+}$ ratio of 5.0. Meanwhile, the XRD patterns derived from Cr^{3+} and In^{3+} exhibited much more peak broadening than those from Al^{3+} and Ga^{3+} . Such low crystallinity of CaIn-LDH seemed to be due to large size of In^{3+} whereas that of CaCr-LDH due to a coordination environment of Cr^{3+} , CrO_4^- rather than CrO_2^- , in spite of its ion size^{19,20} similar to Fe^{3+} . The reactions with both Al^{3+} and Ga^{3+} led to the crystal morphologies almost same to those with Fe^{3+} . On the other hand, the crystals from the reactions with In^{3+} and Cr^{3+} resulted in quite different morphologies; CaIn-LDH as small flakes and CaCr-LDH as tiny particulates (Fig. S4). This is mainly due to the above mentioned chemical properties of these two cations.

Conclusions

Occurrence of post-isomorphic substitution of heterogeneous cations in already crystallized phases has been elucidated in portlandite crystals as evidenced by the transient appearance of metastable phase, the formation of CaM-LDHs at high pH, the sharp shift of suspension pH after phase transition, and the in situ topochemical reaction. Specifically, it offers an innovative route to simplify synthesis processes and to control crystal morphology for CaM-LDHs. Furthermore, it leads to new understanding on the hydration process of calcium aluminate cement, in particular, the formation and transformation of calcium aluminate hydrate phases that had been explained only by the dissolution and re-precipitation reactions.^{15,16} Therefore, the post-isomorphic substitution revealed in this study could make a substantial contribution to many scientific and industrial fields related to clay and cement minerals.

Notes and references

^a Soil Science Laboratory, School of Applied biosciences, Kyungpook National University, Daegu, 702-701, South Korea. Fax: 82 53953 7233 ; E-mail: manpark@knu.ac.kr

^b Materials Research Laboratory, Pennsylvania State University, State College, PA16802, USA. E-mail: komarneni@psu.edu

† Electronic Supplementary Information (ESI) available: [details of any supplementary information available should be included here]. See DOI: 10.1039/b000000x/

References

- The chemistry of clay minerals: Weaver, E.; Pollard, L, D. Elsevier, Amsterdam, 1973. pp. 1-4.
- (a) S. R. J. Oliver, *Chem. Soc. Rev.*, 2009, **38**, 1868; (b) K. Teramura, S. Iguchi, Y. Mizuno, T. Shishido and T. Tanaka, *Angew. Chem. Int. Ed.*, 2012, **51**, 8008.
- J. M. Zen, A. S. Kumar, *Anal. Chem.*, 2004, **76**, 205A.
- A. Vaccari, *Catal. Today*, 1998, **41**, 53-71.
- X. Chen, J. V. Wright, J. M. Conca and L. M. Peurrung, *Environ. Sci. & Technol.*, 1997, **31**, 624.
- Z. P. Xu and G. Q. Lu, *Chem. Mater.*, 2005, **17**, 1055.
- (a) R. Ma., K. Takada, K. Fukuda, N. Iyi, Y. Bando and T. Sasaki, *Angew. Chem. Int. Ed.*, 2008, **47**, 86; (b) R. Ma, J. Liang, X. Liu and T. Sasaki, *J. Am. Chem. Soc.*, 2012, **134**, 19915.
- L. T. Rakov, *GeoChem. Intl.*, 2006, **44**, 1004.
- P. S. Neuhoff and L. S. Ruhl, *Chem. Geo.*, 2006, **225**, 373.

- 10 (a) S. Komarneni, N. Kozai and R. Roy, *J. Mater. Chem.*, 1998, **8**, 1329; (b) M. C. Richardson and P. S. Braterman, *J. Mater. Chem.*, 2009, **19**, 7965.
- 11 L. Poul, N. Jouini and F. Fievet, *Chem. Mater.*, 2000, **12**, 3123.
- 5 12 G. Renaudin and M. Francois, *Acta Cryst. C*, 1999, **55**, 835.
- 13 L. Vieille, I. Rousselot, F. Leroux, J. P. Besse and C. Taviot-Gueho, *Chem. Mater.*, 2003, **15**, 4361.
- 14 J. S. Valente, E. Lima, J. A. Toledo-Antonio, M. A. Cortes-Jacome, L. Lartundo-Rojas, R. Montiel and J. Prince, *J. Phys. Chem. C*, 2010, 10 **114**, 2089-2099.
- 15 N. Ukrainczyk, T. Matusinovic, S. Kurajica, B. Zimmermann and J. Sipusic, *Thermochimica Acta*, 2007, **464**, 7.
- 16 F. P. Glasser, A. Kindness and S. A. Stronach, *Cem. Concr. Res.*, 1999, **29**, 861.
- 15 17 I. Rousselot, C. Taviot-Gueho, F. Leroux, P. Leone, P. Palvadeau and J. P. Besse, *J. Solid State Chem.*, 2002, **167**, 137.
- 18 T. Runcevski, R. E. Dinnebier, O. V. Magdysyuk and H. Pollmann, *Acta Cryst. B*, 2012, **68**, 493.
- 19 S. Galmarini, A. Aimable, N. Ruffray and P. Bowen, *Cem. Concr. Res.*, 2011, **41**, 1330.
- 20 20 Atlas of Eh-pH diagrams, Takeno, N. Geological Survey of Japan Open File Report No.419, National Institute of Advanced Industrial Science and Technology, Japan, 2005.
- 21 (a) J. W. Boclair and P. S. Braterman, *Chem. Mater.*, 1999, **11**, 298; 25 (b) J. W. Boclair, P. S. Braterman, J. Jiang, S. Lou and F. Yarberrry, *Chem. Mater.*, 1999, **11**, 303.

A variety of trivalent cations substitute for Ca^{2+} ions in already crystallized phase of portlandite through in situ topochemical reaction.

